Chapter 5

Photogeneration of Distant Radical Pairs in Aqueous Pyruvic Acid Glasses

Abstract

The $\lambda > 300$ nm photolysis of h_4- or d_4-pyruvic acid aqueous glasses at 77 K yields identical electron magnetic resonance (EMR) spectra arising from distant ($r \geq 0.5$ nm) triplet radical pairs. Spectra comprise: (1) well-resolved quartets, *X*, at $g \sim g_e$ that closely match the powder spectra of spin pairs interacting across $r \sim 1.0$ nm with $D \sim 3.0$ mT, $E \sim 0$ mT zero field splittings (ZFS) and, (2) broad signals centered at $g \sim 2.07$, *Y*, that display marked *g*-anisotropy and *g*-strain, exclude $D \geq 20.0$ mT values (i.e., $r \leq 0.5$ spin nm separations), and track the temperature dependence of related $g \sim 4$ features. These results imply that the n-π^* excitation of pyruvic acid, PA, induces long-range electron transfer from the promoted carbonyl chromophore into neighboring carbonyl acceptors, rather than homolysis into contact radical pairs or concerted decarboxylation into a carbene. Since PA is associated into hydrogen-bonded dimers prior to vitrification, *X* signals arise from radical pairs ensuing intradimer electron transfer to a locked acceptor, while Y signals involve carbonyl groups attached to randomly arranged, disjoint monomers. The ultrafast decarboxylation of primary radical ion pairs, $^3[PA^{+}\cdot\ PA^{-}\cdot]$, accounts for the release of CO_2 under cryogenic conditions, for the lack of thermal hysteresis displayed by magnetic signals between 10–160 K, and for averted charge retrotransfer. All EMR signals disappear irreversibly above the onset of ice diffusivity at ~ 190 K.

Introduction

The organic matter embedded in snow is susceptible to photochemical transformations that ultimately affect the composition of the lower atmosphere.[1,2] The secular photodecarbonylation/decarboxylation of organic dopants in ice cores eventually corrupts paleoatmospheric polar CO/CO_2 records.[3,4] New organic species are produced in both cases. These processes involve the excitation of organic and/or inorganic chromophores in sunlit snowpacks,[5-8] and in deep ice perennially exposed to the ultraviolet Cerenkov radiation generated by penetrating cosmic muons.[4] Carbonyls are the predominant organic chromophores found in snow and ice, and also in the aquatic colored organic matter carried by atmospheric aerosols.[9-12] While the photodegradation of the colored organic matter present in natural waters has been extensively investigated in connection with the geochemical carbon cycle, and with reentry into the microbial food chain,[13-16] the photochemical processing of organic matter in frozen media remains a largely unexplored field.

Upon freezing most polar organic solutes are segregated from pure ice to accumulate in supercooled microfluids or glasses.[17-19] Solute desolvation and/or association becomes the norm in these concentrated liquids.[20,21] The issue is whether factors other than reduced fluidity or the inception of topochemical constraints, such as the state of the solute or the dielectric properties of the solid, affect photochemistry in frozen solutions. We chose to delve into this subject by probing into the location and nature of the paramagnetic intermediates produced in the $\lambda > 300$ nm photolysis of frozen aqueous solutions of pyruvic acid (2-oxopropanoic, PA), a widespread environmental carbonylic

species.[9,10] In water, PA undergoes efficient photodecarboxylation via an excited triplet state, reaction 5-1:[22,23]

$$CH_3C(O)C(O)OH + h\nu \rightarrow\rightarrow {}^3[CH_3C(O)C(O)OH]^* \rightarrow\rightarrow CO_2 + \text{other products} \quad (5\text{-}1)$$

A carbene, 1-hydroxyethylidene, $^3CH_3C(OH)$**:**,[24] or contact radical pairs, $^3[CH_3C(O)\bullet \bullet COOH]$,[25] have been postulated as potential intermediates in reaction 5-1. Kinetic spectroscopy experiments in solvents of varied polarity have demonstrated, however, that the 355 nm photolysis of PA in water proceeds by intermolecular electron transfer between $^3PA^*$ and ground state PA molecules.[26-28] In this paper we report electron magnetic resonance (EMR) spectra of photolyzed PA in ice, and on the kinetics of CO_2 evolution during PA photolysis under cryogenic conditions, which provide information on reactive intermediates, and on the role of long-range photoinduced electron transfer (PET) in aqueous glasses.[29-31]

Experimental Section

200 μL of 0.1 M PA (Aldrich, twice-distilled at reduced pressure) solutions in pure H_2O or D_2O contained in silica tubes (RotoTite, Wilmad, 4 mm o.d.) were degassed via freeze-and-thaw cycles under vacuum, and finally immersed in an unsilvered fused silica dewar filled with liquid N_2. GC-MS analysis of preequilibrated h_4-PA solutions in excess D_2O confirmed the full exchange of all protons into d_4-PA via acid-catalyzed enolization. These samples were irradiated with the output of a 1 kW high-pressure Xe-Hg lamp, after removing unwanted infrared emissions by means of a water filter. A $\lambda = 320 \pm 10$ nm band-pass interference filter (Oriel) was also used in some experiments. After irradiation,

samples were rapidly transferred to the cavity of a Bruker EM X-band cw EMR spectrometer. The temperature of the cavity could be controlled between 10 K and 300 K by a helium cryostat (Oxford). The spectrometer typically operated at 9.377 GHz (center field ~ 335 mT). EMR spectra were processed, analyzed, and simulated using WINEPR SimFonia (Bruker) software. The evolution of CO_2 during the photolysis of frozen PA solutions was studied in a sealed cylindrical photochemical reactor provided with online gas-phase infrared detection, and a lamp immersion well. PA solutions (0.1 M, 4 mL) were sparged with ultrapure N_2 for 30 min, frozen on the reactor walls at 240 K, degassed under vacuum, and finally kept under 1 atm ultrapure N_2 at < 143 K, while being irradiated with a PenRay lamp emitting at 320 nm. The gaseous content of the reactor was circulated, via a micropump, through an infrared gas cell for continuous CO_2 monitoring. The sublimation pressure of neat CO_2 is $p_{CO_2} > 2.5$ hPa above 143 K.

Results and Discussion

EMR spectra, recorded at 20 K and 100 K, of degassed, frozen h_4-PA solutions irradiated for 50 min at 77 K, are shown in Figure 5-1. These spectra were stable for hours: Their appearances and intensities could be recovered after repeated temperature cycles below ~ 180 K. All paramagnetic species irreversibly decayed, however, into diamagnetic products above ~ 190 K in a few minutes. Based on their similar temperature dependences, the broad "Y" signals at $g \geq 2$ and $g \sim 4$ are assigned to a common carrier, which we label $^3RP_1$. The well-resolved "X" features at $g \sim 2$ lack detectable $g \sim 4$ counterparts, and correspond to different species designated as $^3RP_2$. We find that the ratios, β, of the integrated intensities of *Y* signals (in the absorption mode), S_g (T): β(g ~

2) = $S_{g\sim2}$(20K)/$S_{g\sim2}$(100 K) = 7.4, and β(g ~ 4) = $S_{g\sim4}$(20K)/$S_{g\sim4}$(100 K) = 7.1, are identical within experimental error, but significantly larger than β(g ~ 2) = 3.1, for the *X* signal. Deconvolution of the spectra of Figure 5-1 yields the spectrum of $^3RP_2$ shown in Figure 5-2A, and the spectrum of $^3RP_1$ of Figure 5-3.

The presence of a $\Delta M_S = 2$ transition, together with the absence of resolved spectral features attributable to zero field splitting (ZFS) interactions exceeding $D \approx 20$ mT, within the span of the broad band centered at $g \sim 2.07$ in Figure 5-3, indicate that $^3RP_1$ contains triplet correlated spins localized on disjoint atoms. Since D is related to the interspin separation, r, according to Eq. 5-2:[34,35]

$$r = \frac{1.41}{D^{1/3}} \tag{5-2}$$

(r in nm, D in mT) the condition $D \leq 20$ mT translates into $r_1 \geq 0.52$ nm. Triplet carbenes, such as the putative 1-hydroxyethylidene, $^3CH_3C(OH)$**:,** that would be formed in reaction 5-3:

$$^3[CH_3C(O)C(O)OH]^* \rightarrow {}^3CH_3C(OH): + CO_2 \tag{5-3}$$

are excluded as intermediates by the fact that their characteristic D values are an order of magnitude larger.[36,37] The asymmetry of the $^1M_S = 1$ transition about its center at H_{cf} = 324 mT, which lies significantly upfield of the center-field H_{cf} = 314 mT value that could have been inferred from the position of the half-field transition (Figure 5-3), should be ascribed to sizable g-anisotropy. The blurring of spectral features, on the other hand, implies extensive g-strain.

Large g-anisotropy is an indication of strong and directional interactions with the medium.[38] For example, the EMR spectra of ·OH radicals in aqueous glasses display a

broad doublet in the $g_\perp \sim g_e = 2.0023$ region, which extends downfield over the $g_\parallel = g_z \sim$ 2.25–2.05 range.[39] Large ^1g_z shifts are generally due to geometry changes; in the case of triplet radical pairs g-anisotropy may also involve singlet-triplet spin-orbit coupling.[40,41] The EMR spectrum of triplet radical pairs in powdered crystalline materials can be simulated by a randomly oriented ensemble of otherwise identical sites. The description of glassy or disordered solid often requires, however, considering an additional ensemble of sites with differing local environments.[42,43] Thus, radical pairs in glassy systems may give rise to well-defined signals at $g \sim 4$ corresponding to nearly isotropic transitions between similarly perturbed $|\pm 1\rangle$ triplet states, while their $g \sim 2$ features could be extensively broadened, as in the present case, due to a distribution of D values, the parameter that determines the relative energies of the $|0\rangle$ vs. $|\pm 1\rangle$ states,[44] over a range of spin separations.[45]

Despite the absence of complementary $g \sim 4$ signals, the X spectral features shown in Figure 5-2A must be also assigned to magnetic dipole zero field interactions between triplet correlated spin pairs, rather than to nuclear hyperfine splittings (hfs), because: (1) they can be simulated (Figure 5-2B) as the powder spectrum of a $S = 1$ species with $D =$ 2.85 mT, $E = 0.3$ mT, half-width ~ 0.4 mT Gaussian lines, interacting with three neighboring protons inducing $a_H \sim 0.3$ mT hfs that are unresolved at 100 K but become apparent at 20 K (Figure 5-2C) and, more decisively, (2) an identical four-line spectrum is obtained in the photolysis of d_4-PA aqueous glasses (Figure 5-2D) that can be simulated using the same zero field splitting parameters ($D = 2.85$ mT, $E = 0.3$ mT) and $a_D = 0.154\ a_H \sim 0.046$ mT hfs (Figure 5-2E).[34] The $^3RP_2$ radical pairs, $r_2 = 1.0$ nm apart (from Eq. 5-2), are expected to have very weak half-field transitions. Since the intensities

of $^1M_s = 2$ transitions fall off as r^{-3},[46-48] radical pairs separated by more than $r \sim 0.8$ nm fail to exhibit detectable $g \sim 4$ transitions.[45,49] We verified that all signal intensities, S, are proportional to T^{-1} between 20 and 60 K, i.e., that both $^3RP_1$ and $^3RP_2$ obey follow Curie's law and are, therefore, triplet ground states.

Summing up, the above results represent compelling evidence that (1) the detected intermediates are not isolated monoradicals, but triplet-correlated radical pairs whose energy levels are largely determined by anisotropic magnetic dipolar interactions and, (2) both $^3RP_1$ and $^3RP_2$ radical pairs are separated by more than $r \sim 0.5$ nm. These conclusions are robust, i.e., independent of more detailed spectral analysis or simulations, and have definite mechanistic implications.

The fact that CO_2 begins to evolve into the gas phase upon warming up photolyzed PA glasses above ~ 140 K (Figure 5-4), i.e., above the temperature at which the sublimation pressure of CO_2 exceeds ~ 2.5 hPa and becomes detectable in our setup, requires CO_2 to be either a primary photoproduct, or the result of the decomposition of primary intermediates under cryogenic conditions. Since EMR spectra do not display thermal hysteresis below ~ 180 K, we argue that decarboxylation occurs concomitantly with, or immediately after, photon absorption via an essentially barrierless reaction.

Several arguments can be adduced against α-cleavage, reaction 5-4

$$^3[CH_3C(O)C(O)OH]^* \rightarrow {}^3[CH_3C(O)\cdot\ \cdot C(O)OH] \qquad (5\text{-}4)$$

not only as a source of detectable paramagnetic species in our system, but as a viable decarboxylation pathway. The close radical pairs generated by α-cleavage in the photolysis of ketones in polycrystalline ice matrices undergo cage recombination approaching unitary efficiency below ~ 190 K.[18] Contact radical pairs produced in

reaction 5-4 will, therefore, recombine soon after photolysis and escape detection. Furthermore, the fact that ·C(O)OH absorbs weakly at 320 nm ($\lambda_{max} \sim 235$ nm),[50] and its thermal decomposition

$$\cdot C(O)OH \rightarrow CO_2 + H\cdot \qquad (5\text{-}5)$$

is considerably endothermic, $\Delta H_{5\text{-}5} \sim 46$ kJ mol^{-1},[51] eliminates the (5-4 + 5-5) pathway as a source of CO_2. A bimolecular H-transfer reaction between ·C(O)OH and PA, such as that postulated in aqueous solution,[25] is also unlikely under present conditions. The irreversible, concerted extrusion of CO_2 from PA, reaction 5-3, would, of course, circumvent these difficulties, but will lead to 1-hydroxyethylidene, $^3CH_3C(OH)$**:**, as the species bearing the triplet-correlated spins. As discussed above, this possibility must be rejected on the basis of present EMR evidence.

It should be apparent that the derived separations, $r_1 \geq 0.5$ nm, $r_2 \sim 1.0$ nm, so considerably exceed normal covalent bond distances that they could only be achieved, in a rigid matrix under cryogenic conditions, via electron transfer over a static nuclear framework, rather than by displacement of contact radical fragments, such as those that would be produced in reaction (5-4). Moreover, considering that $^3PA^*$ excitation is largely localized onto the carbonyl chromophore, PET should take place between excited ^{3}(C=O)* donors and ground state C=O acceptors, reaction 5-6:

$$^3PA^* + PA \rightarrow {}^3[PA^{+\cdot} + PA^{-\cdot}] \qquad (5\text{-}6)$$

The slow cooling of aqueous solutions leads to pure ice crystals wet by increasingly concentrated fluids. The solute may ultimately separate as a distinct phase only below the eutectic.[52] Cooling rates sufficiently rapid to overcome solute segregation are difficult to achieve, and even more difficult to reproduce.[53] However, upon freezing

aqueous solutions of polar organic compounds, the solute retains a certain amount of water in the form of a supersaturated solution that eventually solidifies as a glass.[33,54,55] Differential scanning calorimetry indeed shows that the solids produced by steadily cooling aqueous PA solutions at 0.5 °C min^{-1} are glasses that display a single endotherm, at the depressed melting point of the solvent, during the warming cycle.[32] Therefore, frozen PA solutions actually consist of a reticular aqueous organic glass microscopically interspersed in a polycrystalline ice matrix. Neither PA remains monomeric in these glasses.[56] The extent of PA dimerization, ~ 5% in 0.1 M PA at 298 K,[57] increases at lower temperatures and higher PA concentrations, and is expected to approach completion a few degrees below the onset of freezing.[21] Thus, in our samples, PA is present as hydrogen-bonded PA dimers randomly distributed within glassy water, in which conjoint monomers are locked in well-defined geometries determined by strong hydrogen-bonding interactions. Intradimer carbonyl-carbonyl distances derived from X-ray difraction studies,[58] or DFT calculations,[59] r_{12} = 0.87 nm, are considerably longer than the closest interdimer carbonyl-carbonyl distances, r_{13} = 0.52 nm, across monomolecular water bridges (see Figure 5-5).

The large excess energies of electronically excited carbonyls (> 300 kJ mol^{-1}) render them more powerful reductants/oxidants than their ground state precursors.[60] ^{3}PA* has an intrinsic lifetime of ~ 0.5 μs in solution and is quenched by PA with a rate constant of k_q ~ 2×10^8 M^{-1} s^{-1}.[26] By assuming: (1) that quenching proceeds via electron transfer during (^{3}PA* + PA) encounters, (2) a rate constant for diffusional encounter, $k_{diff} \sim 4 \times 10^9$ M^{-1} s^{-1} and, (3) ~1 ps encounter lifetimes,[61] we infer an effective electron transfer rate constant, $k^0_{ET} \sim 5 \times 10^{10}$ s^{-1}, upon close contact at r_0 ~ 0.28 nm (i.e., the O-atom van der

Waals diameter). If k_{ET} decays exponentially with separation: $k_{ET} = k^0_{ET} \exp[-\beta(r - r_0)]$, and if β= 16.5 nm^{-1} across water bridges, and β ~8.4 nm^{-1} along the covalent bonds joining the carbonyl donor and acceptor groups in PA dimers,[29-31,62,63] electrons will be competitively transferred from the excited carbonyl, say 1 in Figure 5-5, along the 1 → 2 and 1 → 3 pathways. The photolysis of cryogenic PA aqueous glasses is expected to generate, therefore, radical pairs involving both conjoint and disjoint moieties.

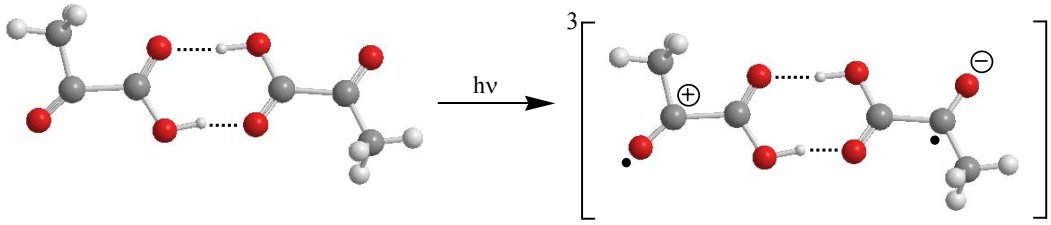

Scheme 5-1

On the basis of the foregoing discussion, we ascribe the well-resolved spectra of Figures 5-2 to the $^3RP_2$ radical pairs produced following intradimer photoinduced electron transfer (Scheme 5-1) while the $^3RP_1$ radical pairs derive from interdimer electron exchange. The initially formed radical ions $PA^{+}\cdot$ and $PA^{-}\cdot$ do not retain their identity. The radical cation, $PA^{+}\cdot$, undergoes ultrafast deprotonation followed by decarboxylation of the resulting acylcarbonyloxyl radicals, reaction 5-7:[64,65]

$$[CH_3C(O)C(O)OH]^{+\bullet} \xrightarrow{-H^+} CH_3C(O)C(O)O\bullet \rightarrow CH_3C(O)\bullet + CO_2 \qquad (5\text{-}7)$$

The relative stabilities of the distonic forms of ketyl radical anions, such as $PA^{-}\cdot$, are known to be sensibly affected by the medium.[66,67] Thus, the C-centered ketyl radical, A, (Scheme 5-2) may coexist with its alkoxyl isomer, B, in ice matrices.

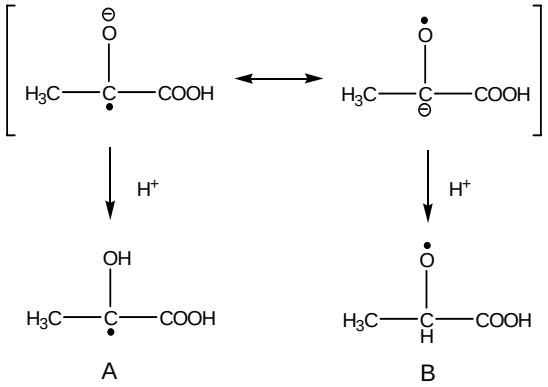

Scheme 5-2

We arrive at the conclusion that the detected ^{3}RP's involve the pairing of acetyl radicals with A or B. While the hyperfine interactions of the acetyl radical are not resolved under 0.5 mT linewidth Gaussian peaks, the larger hfs's of methyl protons in the ketyl radical A: $a_H(3\beta)$ = 1.70 mT [$a_H(1\beta)$ = 0.23 mT, $a_H(1\gamma)$ = 0.10 mT],[68] lead to simulated spectra of strongly electron exchanged (i.e., $J >> a_H$)[34] ^{3}RP's displaying six, rather than four main lines (cf. the simulated spectrum of $^3RP_2$ in Figure 5-2). Thus, experimental spectra may express the more diffuse hyperfine structures associated with the intermediate case: $J \sim a_H$,[69] or the ^{3}RP's actually involve acetyl and the alkoxyl radical B, which has only one $a_H(\beta)$ hfs. Further elaboration is unwarranted. Notice that the actual r separation in $^3RP_2$ radical pairs may exceed r_{12} = 0.87 nm (as in PA dimers, see above) due to the chemical transformations, such as decarboxylation, undergone by primary radical pairs.

Present experiments provide, therefore, direct confirmation that PA photodecarboxylation in aqueous media is initiated by PET rather than by homolytic pathways.[26,27,70]

Acknowledgment: This work was financed by NSF grant ATM-0228140. A. J. Di Bilio provided valuable assistance with EMR experiments.

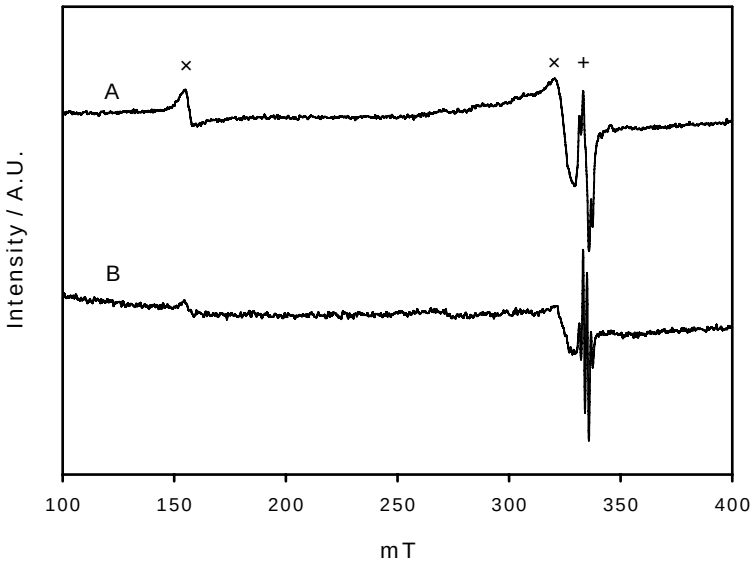

Figure 5-1. EMR spectra of degassed, frozen 0.1 M h_4-PA aqueous solutions previously irradiated at 320 ± 10 nm, 77 K for 50 min, and acquired at: 20 K (A), 100 K (B). X and Y signals are associated with $^3RP_2$ and $^3RP_1$ radical pairs, respectively. See text.

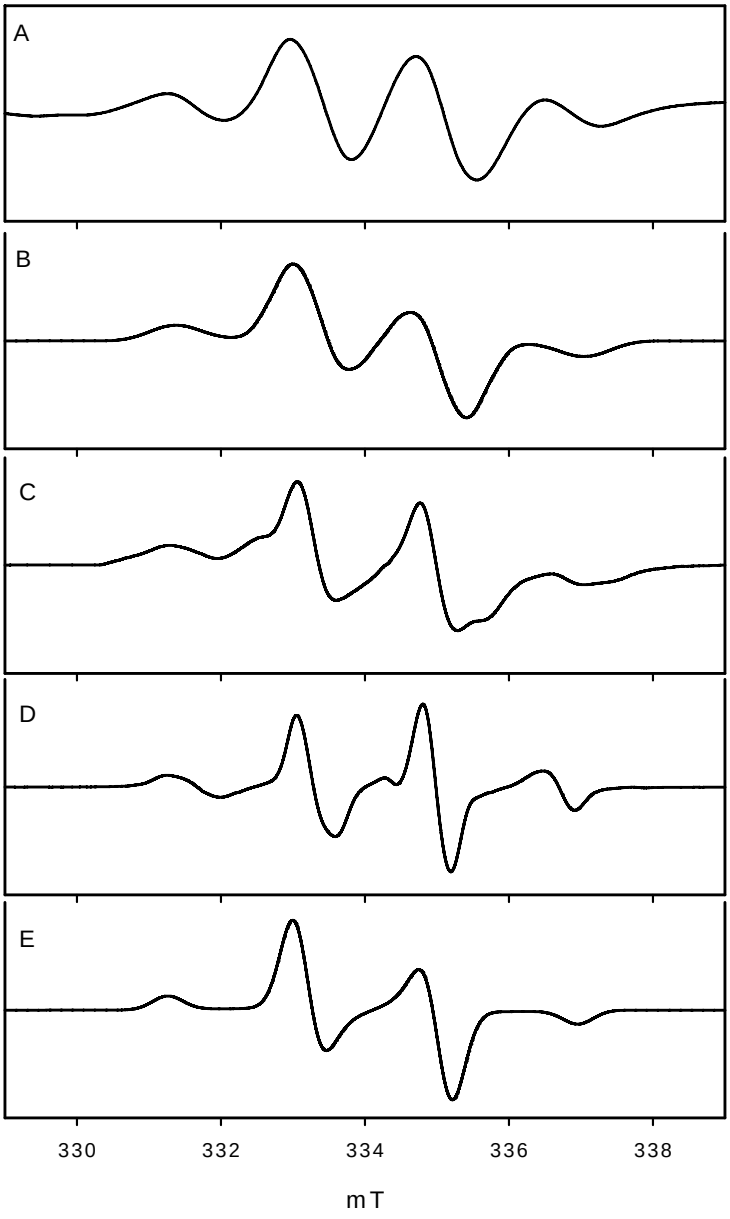

Figure 5-2. EMR spectra of $^3RP_2$ radical pairs. **A**: in photolyzed h_4-PA, at 100 K. **B**: the **A** spectrum simulated as the powder spectrum of a $S = 1$ species, with $D = 2.85$ mT, $E = 0.30$ mT, $a_H(3) = 0.3$ mT, $g = 2.006$, 0.4 mT Gaussian linewidths. **C**: in photolyzed h_4-PA, at 20 K. **D**: in photolyzed d_4-PA, at 100 K. **E**: the **D** spectrum simulated as the powder spectrum of a $S = 1$ species, with $D = 2.85$ mT, $E = 0.30$ mT, $a_D(3) = 0.046$ mT, $g = 2.006$, 0.4 mT Gaussian linewidth.

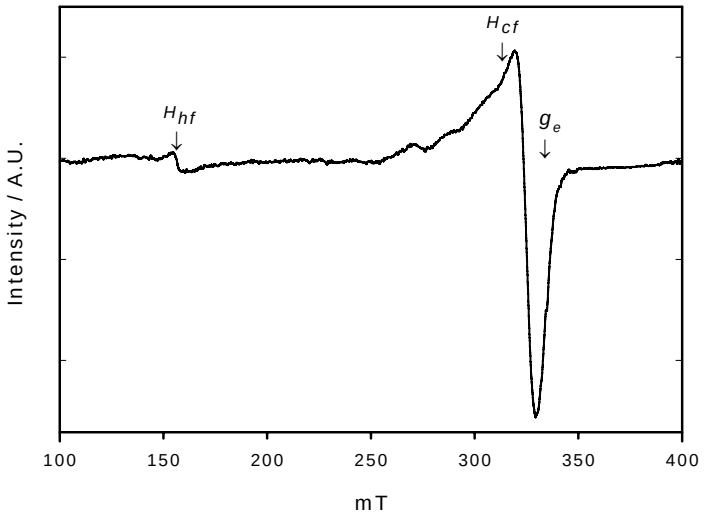

Figure 5-3. The EMR spectrum of $^3RP_1$ radical pairs, deconvoluted from Fig. 5-1

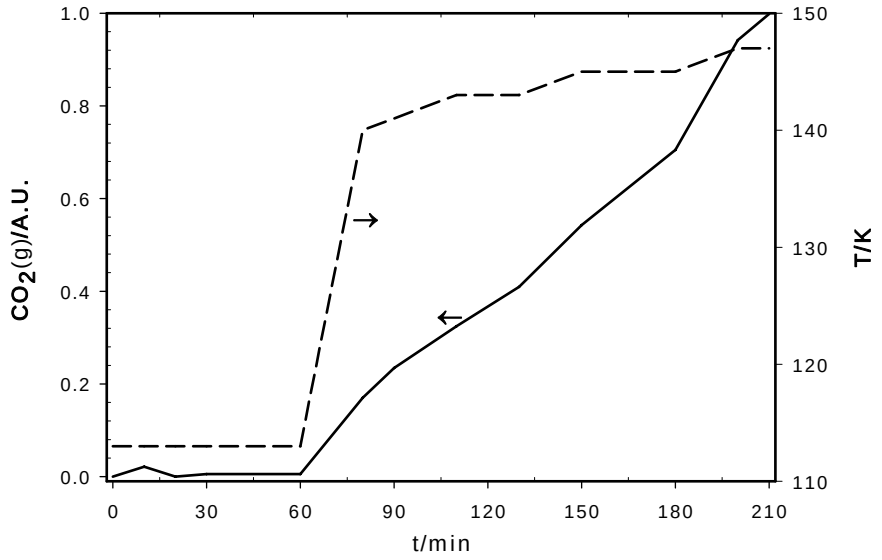

Figure 5-4. CO_2(g) released during the λ = 320 nm photolysis of deareated, frozen 0.1 M *h*$_4$-PA solutions (solid line, left axis). Sample temperature (dashed line, right axis). P_{CO_2} < 1 hPa at T < 130 K.

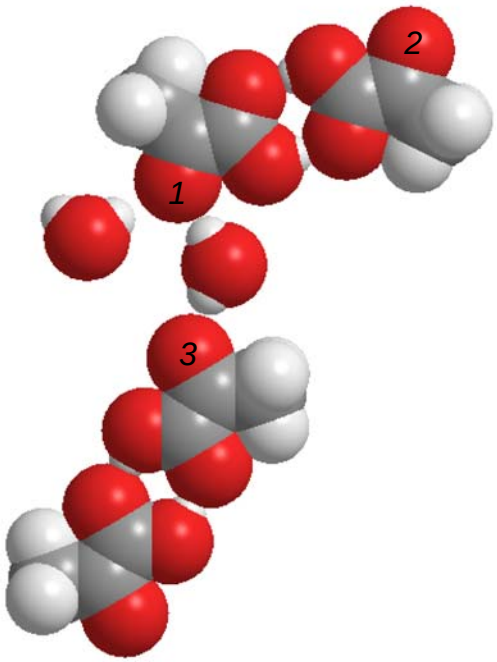

Figure 5-5. Pyruvic acid dimers embedded in water ice.

References

1- Domine, F.; Shepson, P. B. *Science* **2002**, *297*, 1506.

2- Honrath, R. E.; Peterson, M. C.; Guo, S.; Dibb, J. E.; Shepson, P. B.; Campbell, B. *Geophys. Res. Lett.* **1999**, *26*, 695.

3- Ahn, J.; Wahlen, M.; Deck, B. L.; Brook, E. J.; Mayewski, P. A.; Taylor, K. C.; White, J. W. C. *J. Geophys. Res.* **2004**, *109*, D13305.

4- Colussi, A. J.; Hoffmann, M. R. *Geophys. Res. Lett.* **2003**, *30*, 1195.

5- Dubowski, Y.; Boxe, C. S.; Colussi, A. J.; Hoffmann, M. R. *J. Phys. Chem. A* **2002**, *106*, 6967.

6- Dubowski, Y.; Colussi, A. J.; Hoffmann, M. R. *J. Phys. Chem. A* **2001**, *105*, 4928.

7- Burkhart, J. F.; Hutterli, M.; Bales, R. C.; McConnell, J. R. *J. Geophys. Res.* **2004**, *109*, D19302.

8- Li, S. M.; Winchester, J. W. *Geophys. Res. Lett.* **1993**, *20*, 45.

9- Kawamura, K.; Imai, Y.; Barrie, L. A. *Atmos. Environ.* **2005**, *39*, 599.

10- Kawamura, K.; Yokoyama, K.; Fujii, Y.; Watanabe, O. *J. Geophys. Res.* **2001**, *106*, 1131.

11- Grannas, A. M.; Shepson, P. B.; Filley, T. R. *Global Biogeochemical Cycles* **2004**, *18*, GB1006.

12- Grannas, A. M.; Shepson, P. B.; Guimbaud, C.; Sumner, A. L.; Albert, M.; Simpson, W.; Domine, F.; Boudries, H.; Botthenheim, J.; Beine, H. J.; Honrath, R.; Zhou, X. *Atmos. Environ.* **2002**, *36*, 2733.

13- Miller, W. M.; Zepp, R. G. *Geophys. Res. Lett.* **1995**, *22*, 417.

14- Mopper, K.; Zhou, X.; Kieber, R. J.; Sikorski, R. G.; Jones, R. D. *Nature* **1991**, *353*, 60.

15- Valentine, R. L.; Zepp, R. G. *Environ. Sci. Technol.* **1993**, *27*, 409.

16- Osburn, C. L.; Morris, D. P.; Thorn, K. A.; Moeller, R. E. *Biogeochemistry* **2001**, *54*, 251.

17- Boxe, C. S.; Colussi, A. J.; Hoffmann, M. R.; Tan, D.; Mastromarino, J.; Sandholm, S. T.; Davies, D. D. *J. Phys. Chem. A* **2003**, *107*, 11409.

18- Ruzicka, R.; Barakova, L.; Klan, P. *J. Phys. Chem. B* **2005**, *109*, 9346.

19- Cho, H.; Shepson, P. B.; Barrie, L. A.; Corwin, J. P.; Zaveri, R. *J. Phys. Chem. B* **2002**, *106*, 11226.

20- Steiner, T. *Angew. Chem. Int. Ed.* **2002**, *41*, 48.

21- Heger, D.; Jirkovsky, J.; Klan, P. *J. Phys. Chem. A* **2005**, *109*, 6702.

22- Budac, D.; Wan, P. *J. Photochem. Photobiolog. A: Chem.* **1992**, *67*, 135.

23- Wan, P.; Budac, D. *CRC Handbook of Organic Photochemistry and Photobiology*: CRC Press: Boca Raton, 1995.

24- Leermakers, P. A.; Vesley, G. F. *J. Am. Chem. Soc.* **1963**, *85*, 3776.

25- Closs, G. L.; Miller, R. J. *J. Am. Chem. Soc.* **1978**, *100*, 3483.

26- Davidson, R. S.; Goodwin, D.; Fornier de Violet, P. *Chem. Phys. Lett.* **1981**, *78*, 471.

27- Davidson, R. S.; Goodwin, D. *J. Chem. Soc. Perk. Trans. II* **1982**, 1559.

28- Davidson, R. S.; Goodwin, D.; Pratt, J. E. *J. Chem. Soc. Perk. Trans. II* **1983**, 1729.

29- Wenger, O. S.; Leigh, B. S.; Villahermosa, R. M.; Gray, H. B.; Winkler, J. R. *Science* **2005**, *307*, 99.

30- Wenger, O. S.; Gray, H. B.; Winkler, J. R. *Chimia* **2005**, *59*, 94.

31- Gray, H. B.; Winkler, J. R. *Proc. Natl. Acad. Sci. USA* **2005**, *102*, 3534.

32- Guzman, M. I.; Colussi, A. J.; Hoffmann, M. R. *Unpublished results*.

33- Franks, F. *Water, a Comprehensive Treatise*; Plenum Press: New York, 1982; Vol. 7.

34- Weil, J. A.; Bolton, J. R.; Wertz, J. E. *Electron Paramagnetic Resonance: Elementary Theory and Practical Applications*; Wiley: New York, 1994.

35- Gordy, W.; Morehouse, R. *Phys. Rev.* **1966**, *151*, 207.

36- Dougherty, D. A. *Kinetics and Spectroscopy of Carbenes and Biradicals*; Platz, M. S., Ed.; Plenum: New York, 1990; pp 117.

37- Tomioka, H. *Reactive Intermediate Chemistry*; Wiley-Interscience: New York, 2004.

38- Lassmann, G.; Kolberg, M.; Bleifuss, G.; Graslund, A.; Sjoberg, B. M.; Lubitz, W. *Phys. Chem. Chem. Phys.* **2003**, *5*, 2442.

39- Riederer, H.; Huttermann, J.; Boon, P.; Symons, M. C. R. *J. Magn. Reson.* **1983**, *54*, 54.

40- Pashenko, S. V.; Proskuryakov, I. I.; Germano, M.; van Gorkom, H. J.; Gast, P. *Chem. Phys.* **2003**, *294*, 439.

41- Zeng, R.; Budil, D. E. *Chem. Phys.* **2003**, *294*, 347.

42- Taylor, P. C.; Baugher, J. F.; Kriz, H. M. *Chem. Rev.* **1975**, *75*, 203.

43- Griscom, D. L.; Taylor, P. C.; Ware, D. A.; Bray, P. J. *J. Chem. Phys.* **1968**, *48*, 5158.

44- Bauld, N. L. *Radicals, Ion Radicals and Triplets*; Wiley-VCH: New York, 1997.

45- Harrison, N.; Symons, M. C. R. *J. Chem. Soc. Faraday Trans.* **1993**, *89*, 59.

46- Eaton, S. S.; Moore, K. M.; Swant, B. M.; Eaton, G. R. *J. Am. Chem. Soc.* **1983**, *105*, 6560.

47- Eaton, S. S.; Eaton, G. R. *J. Am. Chem. Soc.* **1982**, *104*, 5002.

48- Eaton, S. S.; Eaton, G. R. *Distance Measurements in Biological Systems by EPR*; Kluwer Academic/Plenum: New York, 2000; Vol. 19.

49- Bednarek, J.; Plonka, A.; Hallbrucker, A.; Mayer, E.; Symons, M. C. R. *J. Am. Chem. Soc.* **1996**, *118*, 9387.

50- Neta, P.; Simic, M.; Hayon, E. *J. Phys. Chem.* **1969**, *73*, 4207.

51- Lissianski, V.; Yang, H.; Qin, Z.; Mueller, M. R.; Shin, K. S.; Gardiner, W. C. *Chem. Phys. Lett.* **1995**, *240*, 57.

52- Reisman, A. *Phase Equilibria*; Academic Press: New York, 1970.

53- Leigh, J. S.; Reed, G. H. *J. Phys. Chem.* **1971**, *75*, 1202.

54- Angell, C. A. Supercooled water. In *Water, a Comprehensive Treatise*; Franks, F., Ed.; Plenum: New York, 1982; Vol. 7 Ch. 1.

55- Cai, Z.; Sevilla, M. D. *Top. Curr. Chem.* **2004**, *237*, 103.

56- Génin, F.; Quilès, F.; Burneau, A. *Phys. Chem. Chem. Phys.* **2001**, *3*, 932.

57- Barcza, L.; Mihalyi, K. *Z. Physik. Chem. Neue Folge* **1977**, *104*, 213.

58- Harata, K.; Sakabe, N.; Tanaka, J. *Acta Cryst.* **1977**, *B*, 210.

59- Yang, X.; Orlova, G.; Zhou, X. J.; Leung, K. T. **2003**, *380*, 34.

60- Buchachenko, A. L. *Pure Appl. Chem.* **2000**, *72*, 2243.

61- Step, E. N.; Buchachenko, A. L.; Turro, N. J. *J. Org. Chem.* **1992**, *57*, 7018.

62- Paddon-Row, M. N. *Adv. Phys. Org. Chem.* **2003**, *38*, 1.

63- Cukier, R. I.; Nocera, D. G. *Annu. Rev. Phys. Chem.* **1998**, *49*, 337.

64- Abel, B.; Assmann, J.; Buback, M.; Grimm, C.; Kling, M.; Schmatz, S.; Schroeder, J.; Witte, T. *J. Phys. Chem. A* **2003**, *107*, 9499.

65- Bockman, T. M.; Hubig, S. M.; Kochi, J. K. *J. Org. Chem.* **1997**, *62*, 2210.

66- Chahma, M.; Li, X.; Phillips, J. P.; Schwartz, P.; Brammer, L. E.; Wang, Y.; Tanko, J. M. *J. Phys. Chem. A* **2005**, *109*, 3372.

67- Buckel, W. *FEBS Lett.* **1996**, *389*, 20.

68- Fischer, H.; Paul, H. *Magnetic Properties of Free Radicals*; Springer-Verlag: Berlin-Heidelberg, 1977; Vol. 9.

69- Atherton, N. M.; *Principles of Electron Spin Resonance*; Ellis Horwood: PTR Prentice Hall: New York, 1993.

70- Davidson, R. S.; Goodwin, D.; Turnock, G. *Tetrahedron Lett.* **1980**, *21*, 4943.

Supporting Information

Aqueous d_4-PA solutions were prepared by exchanging 0.1 M solutions of h_4-PA in D_2O at pH 1.0. Pyruvic acid can exchange *all* protons via acid-catalyzed enolization.[‡] Full isotope exchange was confirmed by HPLC analysis of h_4-PA/D_2O solutions that had been prepared at least one month in advance, using electrospray ionization mass spectrometry detection (ESI MS Agilent 1100 series) in the negative ion mode (Figure 5-6).

[‡] Chiang, Y.; Kresge, A. J.; Pruszynski, P. *J. Am. Chem. Soc*. **1992**, *114*, 3103.

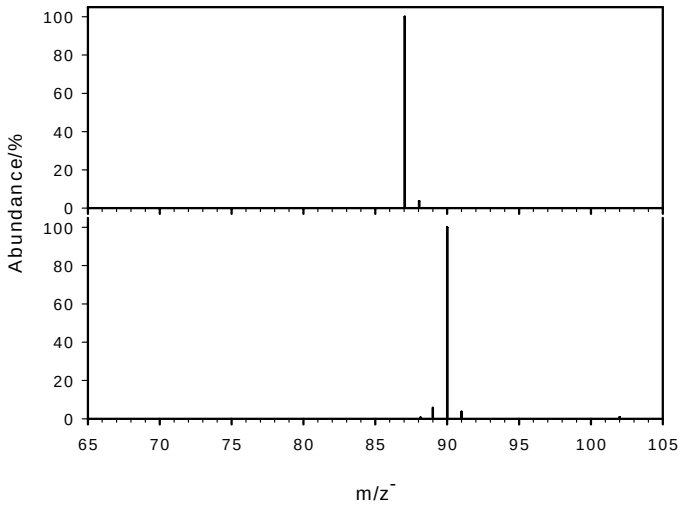

Figure 5-6